


## ORIGINAL ARTICLE

# FHL1: A novel diagnostic marker for papillary thyroid carcinoma

Yeting Zeng<sup>1</sup>  | Dehua Zeng<sup>1</sup> | Xingfeng Qi<sup>1</sup> | Hanxi Wang<sup>2</sup> |  
Xuzhou Wang<sup>1</sup> | Xiaodong Dai<sup>1</sup> | Lijuan Qu<sup>1</sup>

<sup>1</sup>Department of Pathology, Joint Logistic Support Force 900th Hospital, Fuzhou, China

<sup>2</sup>Department of clinical pathology, Medical Research Center, Fujian Medical University, Fuzhou, China

## Correspondence

Yeting Zeng and Lijuan Qu, Department of Pathology, Joint Logistic Support Force 900th Hospital, Fuzhou 350003, China.  
Email: 492077897@qq.com and qjjuan6516@sina.com

## Funding information

Fujian Province clinical key specialty construction project, Grant/Award Number: 2015ZDZKBL

## Abstract

Although there are clear morphologic criteria for the diagnosis of papillary thyroid carcinoma (PTC), when the morphology is untypical or overlaps, accurate diagnostic indicators are necessary. Since few studies investigated the role of down-regulated genes in PTC, this article aims to further explore the molecular markers associated with PTC. We conducted bioinformatics analysis of gene microarrays of PTC and normal adjacent tissues. Besides, quantitative real-time quantitative polymerase chain reaction array and immunohistochemical staining were used to investigate the expression of the major down-regulated genes. The results indicated that several important down-regulated genes, including TLE1, BCL2, FHL1, GHR, KIT, and PPARGC1A were involved in the process of PTC. Compared to normal adjacent tissues, the mRNA expression of the major genes was down-regulated in PTC ( $p < 0.05$ ). Immunohistochemically, FHL1 shows negative or low expression in PTC tissues ( $p < 0.05$ ). BCL2 did not show a significant difference between PTC and normal thyroid tissues ( $p > 0.05$ ). TLE1, KIT, PPARGC1A and GHR showed negative expression in both tumor and normal tissues. These results suggested that FHL1 could serve as a novel tumor marker for precise diagnosis of PTC.

## KEYWORDS

bioinformatics analysis, biomarker, down-regulated DEGs, FHL1, PTC

## INTRODUCTION

Papillary thyroid carcinoma (PTC) is the most prevalent type of thyroid cancer, accounting for over 85% of all thyroid malignancies.<sup>1</sup> Over recent decades, the global incidence of PTC has risen significantly.<sup>2–4</sup> While PTC is typically indolent, it can occasionally exhibit aggressive behaviors, such as metastasis and local recurrence.<sup>3,4</sup> Accurate identification and diagnosis of

thyroid nodules are crucial for distinguishing tumors with aggressive characteristics.

Contemporary research on the molecular pathogenesis of PTC has primarily concentrated on genetic alterations that are highly expressed across various signaling pathways.<sup>4</sup> PTC exhibits several variants characterized by mutually exclusive mutations that primarily affect the mitogen-activated protein kinase pathway, essential for PTC progression.<sup>5,6</sup> the BRAF V600E

**Abbreviations:** DEGs, differentially expressed genes; FHL1, four and a half LIM domains 1; FNA, fine-needle aspiration; GO, gene ontology; GSEA, gene set enrichment analysis; NIFTP, noninvasive follicular thyroid neoplasm with papillary-like features; PTC, papillary thyroid carcinoma; Q-PCR, quantitative real-time quantitative polymerase chain reaction; TCGA, The Cancer Genome Atlas Program.

Yeting Zeng and Dehua Zeng are contributed equally to this study.

This is an open access article under the terms of the [Creative Commons Attribution-NonCommercial-NoDerivs](https://creativecommons.org/licenses/by-nc-nd/4.0/) License, which permits use and distribution in any medium, provided the original work is properly cited, the use is non-commercial and no modifications or adaptations are made.

© 2024 The Author(s). *Pathology International* published by Japanese Society of Pathology and John Wiley & Sons Australia, Ltd.

mutation is the most common, present in 60% of cases, followed by RAS mutations (15%) and chromosomal rearrangements affecting genes like BRAF or receptor tyrosine kinases such as RET, NTRK, and ALK (12%). The remaining 13% of cases have no known driver mutations.<sup>1</sup> Numerous studies have explored biomarkers critical for tumorigenesis and prognosis in PTC. Established markers include TTF-1, involved in thyroid cell differentiation, and BRAF, whose mutations promote tumorigenesis and are associated with poor prognosis.<sup>7</sup> Other markers such as PAX-8,<sup>8</sup> thyroperoxidase, CK19, galectin-3, FN1,<sup>9</sup> CD56,<sup>10</sup> and HBME-1 are upregulated in PTC compared to normal thyroid tissues. However, the diagnostic reliability of these markers is variable, and they lack specificity for PTC.<sup>11</sup> Additionally, the expressions of CK19, TPO, HBME-1, and galectin-3 do not significantly aid in distinguishing PTC from other aggressive lesions.<sup>12</sup>

Therefore, in this study, we aimed to identify molecular biomarkers that can serve as reliable indicators specifically related to the oncogenesis and progression of PTC.

## METHODS AND MATERIALS

### Patients

This study analyzed 30 archival paraffin-embedded blocks histologically diagnosed as PTC, collected from January 2015 to December 2016. These cases were surgically treated at the Department of General or Head and Neck Surgery at Joint Logistic Support Force 900th Hospital, Fuzhou. Each patient underwent thyroidectomy, with surgical specimens fixed in 10% buffered formalin and diagnosed histopathologically by the Department of Pathology. Clinical and pathological data from these 30 patients were retrospectively reviewed (Table 1), comprising 19 women (63.3%) and 11 men (36.7%), with an average age of  $44.8 \pm 14.7$  years.

### Datasets and data preprocessing

We investigated the gene expression profile of PTC samples by searching the NCBI Gene Expression Omnibus (GEO) (<http://www.ncbi.nlm.nih.gov/geo>). Two datasets based on GPL570, including the GSE3678 dataset from New York Medical School and the GSE33630 dataset from the Free University of Brussels, were downloaded for further research. These datasets were chosen based on their comprehensive inclusion of PTC and corresponding normal tissues-essential for our analysis-and their extensive citation in prior research, affirming their reliability and scientific relevance. We analyzed 7 PTC and adjacent normal samples from GSE3678, alongside 49 PTC and

**TABLE 1** Clinical, and histopathological characteristics of patients with papillary thyroid carcinoma (classical subtype).

Variables	Average $\pm$ SD or number (%)
Age (years)	44.8 $\pm$ 14.7
<45	31.93 $\pm$ 7.2
$\geq$ 45	57.67 $\pm$ 6.2
Gender	
Female	19 (63.3)
Male	11 (36.7)
Multifocality	
Single	17 (56.7)
Multiple	13 (43.3)
pT stage <sup>a</sup>	
pT1a	11 (36.7)
pT1b	3 (10.0)
pT2	9 (30.0)
pT3	7 (23.3)
pT4	0 (0)
FHL1 expression	
Positive	0 (0)
Negative	30 (100)
BCL2 expression	
Positive	28 (93.3)
Negative	2 (6.7)
TLE1, KIT, PPARGC1A, and GHR expression	
Positive	0 (0)
Negative	0 (0)

Abbreviation: FHL1, four and a half LIM domains 1.

<sup>a</sup>pT classification according to the 7th edition of the AJCC cancer staging.

45 normal thyroid samples from GSE33630. Differentially expressed genes (DEGs) were identified through fold-change filtering, using a threshold of  $\log_2FCI$  (Fold Change)  $\geq$  1.5 and an adjusted  $p < 0.01$  to ascertain significant differential expression.<sup>13</sup>

Pathway and Gene Ontology (GO) analysis were conducted to assess the biological functions of this subset of DEGs ( $p < 0.01$ ). Simultaneously, we utilized BioGenet to visualize the protein-protein interaction (PPI) network of DEGs, and filtered the network by calculating the value of all the nodes, which was carried out by Degree-sorting. The hub genes are core genes with important physiological functions. DEGs between Low- and high four and a half LIM domains 1 (FHL1) expression groups were identified by using the DESeq. 2 R package. In this study, Gene Set Enrichment

Analysis (GSEA) was performed using the TCGAplot R package to demonstrate the significant functions and pathways between the two groups.

## ONCOMINE analysis

The ONCOMINE gene expression array datasets ([www.oncomine.org](http://www.oncomine.org)) provide a platform for analyzing the mRNA levels of the hub genes. It is an online cancer microarray database that can facilitate genetic screening through genome-wide expression analyses.<sup>14</sup> In this study, the gene expression datasets of human malignant and normal thyroid tissues were compared using a Student's *t*-test to generate a *p* Value. The *p* Value was set at 0.05, and the fold change was defined as 2. The data type in the datasets was restricted to mRNA.

## Quantitative real-time polymerase chain reaction (Q-PCR)

Total RNA was extracted from consecutive paraffin slices using AmoyDx<sup>®</sup> DNA and RNA Extraction Kits Silica-based Spin Column Reagent (Amoy Diagnostics Co.). Subsequently, the RNA was converted to cDNA using the Primescript RT reagent kit (Takara Bio) following the manufacturer's protocol. Q-PCR was performed using SYBR Premix Ex Taq (Takara Bio) in the Applied Biosystems StepOne Real-Time PCR System (Applied Biosystems). The  $\beta$ -actin gene was used as internal control. The comparative  $C_t$  method was used to quantify gene expression.<sup>15</sup> The target gene expression level was normalized to the expression of the housekeeping gene  $\beta$ -actin within the same sample ( $-\Delta C_t$ ), where the relative expression of each gene was calculated with  $10^3 \times 2^{-\Delta C_t}$ .

## Histopathological examination

All the hematoxylin and eosin stain (H&E) sections were assessed by two independent pathologists to confirm the diagnosis of PTC. All cases were classical forms of PTC without any histological variants. The histological diagnosis of PTC was based on the criteria of the 2017 WHO classification of tumours of endocrine organs.<sup>16,17</sup> These criteria include nuclear features such as: enlargement, crowding, and overlapping, irregularity of nuclear contours, nuclear grooves, ground-glass nuclei characteristics, pseudoinclusions in the nucleus and psammoma bodies. In addition, the classical-type PTC showed characteristic papillary architecture, either pure or mixed with follicles in varying percentages.<sup>16</sup>

## Immunohistochemistry (IHC)

The paraffin tissue blocks were sectioned into 4  $\mu$ m-thick slices and then transferred onto adhesive slides for IHC analysis. Tissue sections were deparaffinized in xylene three times for 5 min each, and then rehydrated in 100%, 95%, 80%, and 75% ethanol for 3 min respectively after overnight incubation at 60°C. Antigen retrieval was performed in a pressure cooker (Supor) for 3 min using x1 citrate buffer (pH 6.0) or EDTA buffer (pH 9.0). Slides were immunostained with monoclonal antibodies against the BCL2 antigen (clone SP66, Maixin), CD117/C-kit antigen (clone YR145, Maixin), and with monoclonal antibodies against the FHL1 (10991-1-AP, Proteintech Group, Inc.), PPARGC1A (Boster, China), and TLE1 antigen (Maixin). The IHC staining was performed using an Envision Plus System (Fuzhou Maixin Biotech Co., Ltd.) according to the manufacturer's protocol.<sup>18</sup> Finally, all the slides were counterstained with hematoxylin. Appropriate positive and negative controls were prepared. The immunostaining scores were assigned by two pathologists using an Olympus BX-51 light microscope (Olympus). Scoring was conducted semi-quantitatively, based on the cytoplasmic staining for BCL2 and FHL1. The staining intensity was graded on a scale of 0 to 3, where 0, 1+, 2+, and 3+ indicate no staining, weak/slight staining, moderate staining, and intense staining respectively. The proportion of positive, immunoreactive tumor cells was interpreted as 1+ (<5% of cells), 2+ (5%–50% of cells), and 3+ (>50% of cells).<sup>11,19</sup> The proportional score and the intensity score were multiplied to obtain a total score, ranging from 0 to 9. Sections with total scores  $\leq 2$  were considered negative, while those with total scores  $\geq 3$  were considered positive.<sup>19</sup>

Written informed consent for the study using these samples was obtained from the patients and approved by the Ethics Committee of 900th Hospital of PLA.

## Statistical analysis

Statistical analysis was conducted using SPSS version 20 software. The chi-square test was used for immunohistochemical analysis of the clinical specimens.

## RESULTS

### GO and pathway analysis for DEGs between PTC and normal thyroid tissues

Differential expression analysis was conducted using Bayes *t*-statistics within the linear models for microarray data (Limma), facilitated by the Bioconductor limma package. DEGs were deemed significant if they met both criteria: an adjusted *p* Value of <0.01 and a  $\log_2$ FCI (fold change)  $\geq 1.5$ . Upon merging datasets

GSE3678 and GSE33630, we identified 429 genes that were significantly altered in PTC tissues compared to normal thyroid tissues. Hierarchical clustering analysis revealed 237 genes were upregulated and 192 genes were downregulated (Figure 1a).

This study primarily focuses on the down-regulated genes in PTC, which have been less frequently reported in existing literature. Significant pathway and GO analyses for these down-regulated genes highlighted associations with thyroid hormone biosynthesis and amino acid metabolism between the PTC and normal thyroid tissue groups (Figure 1b,c).

## Biological functions and pathway analysis of FHL1

To further elucidate the biological functions of FHL1, we analyzed the DEGs between the low- and high-expression FHL1 groups based on the median FHL1 expression value in The Cancer GenomeAtlas Program (TCGA) data thyroid cancer expression profile (Figure 2a). We also conducted a GSEA pathway analysis. The results showed

that high FHL1 expression was mainly enriched in adaptive immune response, lymphocyte-mediated immunity, T cell-mediated immunity, and cell killing (Figure 2b).

## PPI network for the down-regulated DEGs

To further investigate the interactions among down-regulated DEGs in PTC, we utilized BisoGenet software to construct a PPI network. This network elucidates direct or indirect connections among the proteins encoded by these genes. The network comprised 552 nodes and 952 edges, indicating a robust set of predicted functional associations among the proteins (Figure 3a). Additionally, we identified a core network centered around six proteins corresponding to six pivotal hub genes: TLE1, BCL2, FHL1, GHR, KIT, and PPARGC1A. Each of these proteins had more than twenty connections to other proteins in the network, with a node degree cutoff set at 25 (Figure 3b). This core network underscores the significant roles these hub genes play in modulating the tumor biology of PTC through their influence on down-regulated DEGs.

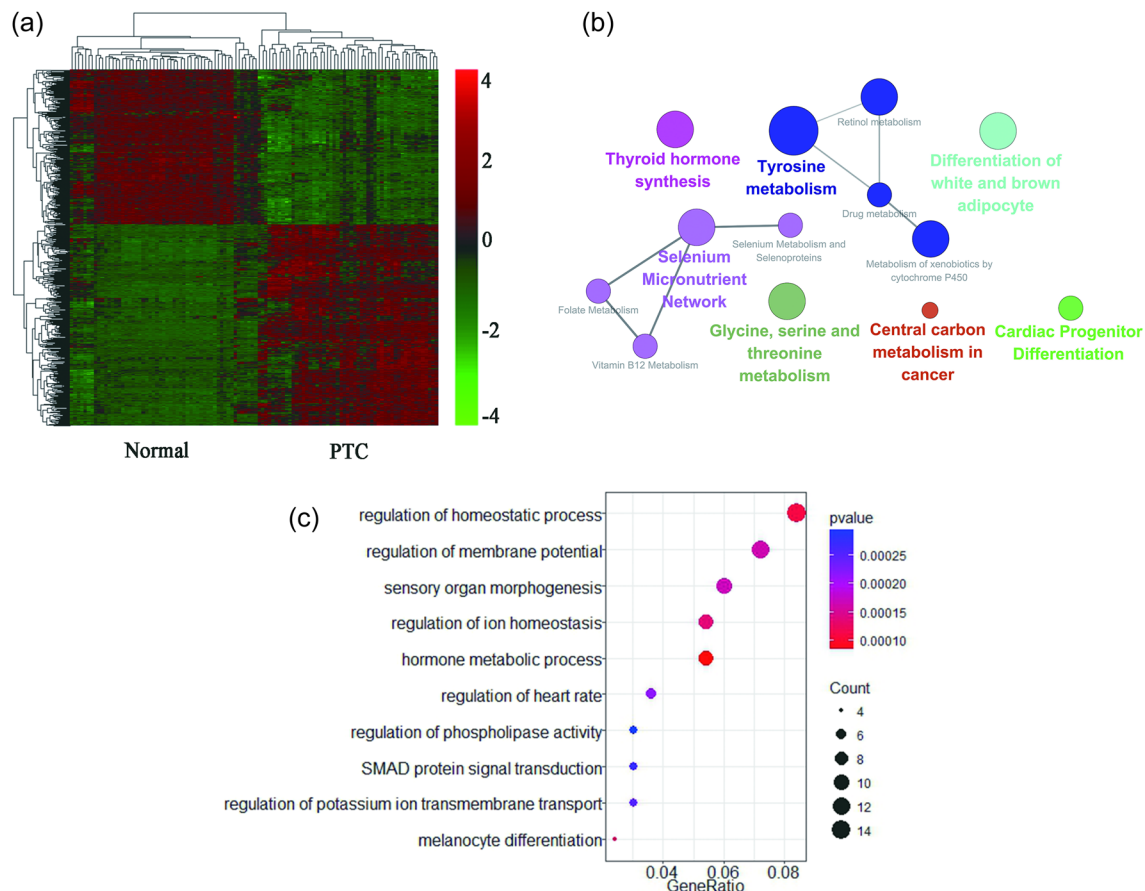


**FIGURE 1** Analysis on the down-regulated differentially expressed genes (DEGs) in Papillary thyroid carcinoma (PTC). (a) Gene expression and cluster analysis of PTC and normal tissues adjacent to cancer. Red represents a high expression while green represents a low expression.  $\log_2FCI$  (Fold Change)  $\geq 1.5$  and adjusted  $p$  Value  $< 0.01$ . (b) Pathway analysis for down-regulated DEGs ( $p$  Value  $< 0.01$ ). (c) Gene Ontology (GO) analysis for down-regulated DEGs ( $p$  Value  $< 0.01$ ).

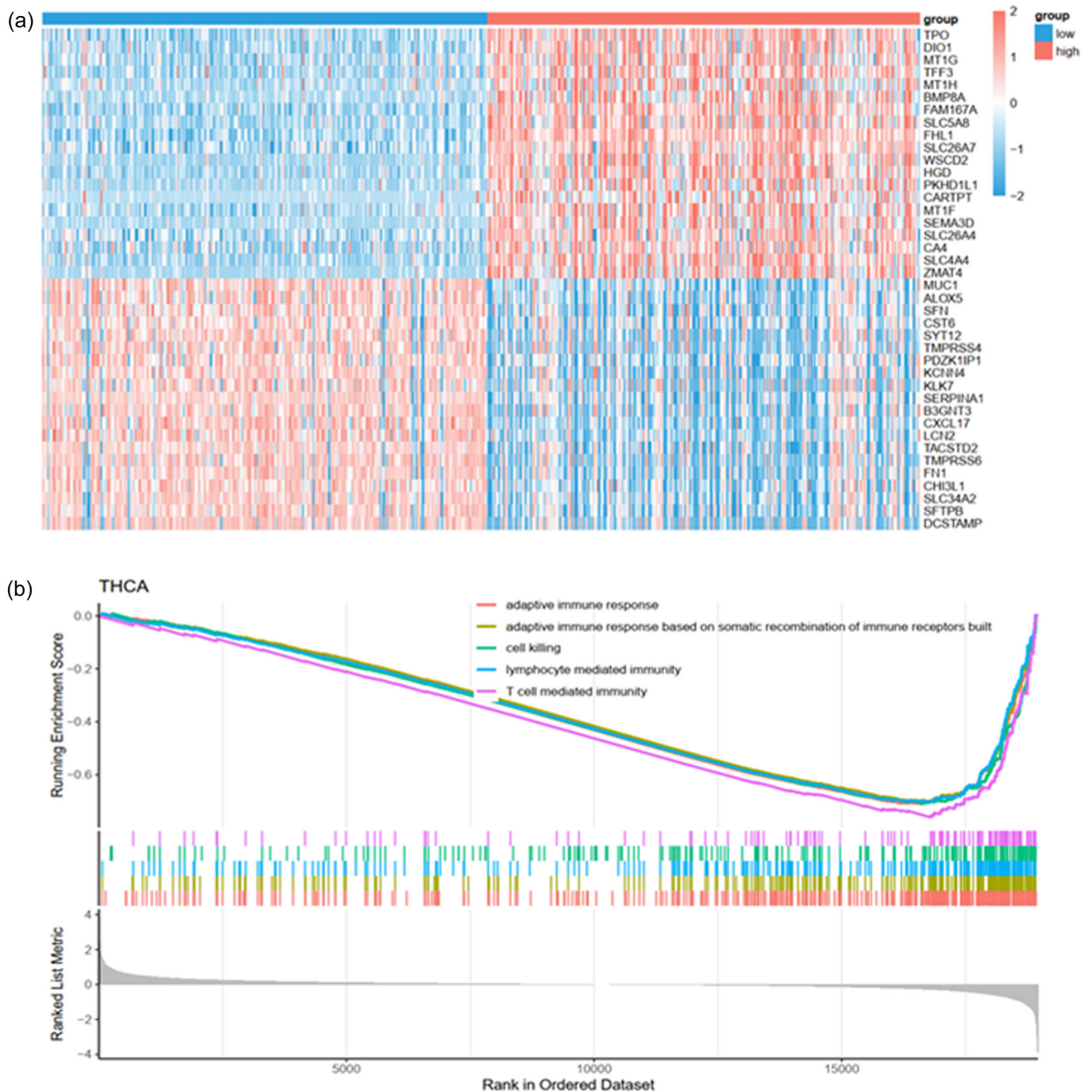


**FIGURE 2** Biological functions and pathway analysis of FHL1. (a) Top20 DEGs between high and low expression groups of FHL1 in TCHA. (b) Enrichment of genes in the representative pathways by GSEA function analysis. DEGs, differentially expressed genes; FHL1, four and a half LIM domains 1; GSEA, Gene Set Enrichment Analysis.

### mRNA expression of six hub genes

To validate the results of microarray data, six selected hub genes (TLE1, BCL2, FHL1, GHR, KIT, and PPARGC1A) were analyzed using ONCOMINE and quantitative real-time PCR. The results are presented in (Figure 4a–f). All six genes showed downregulated in PTC compared with the normal thyroid follicles surrounding the tumour, confirming the results of the microarray

analysis (Figure 4g–l). By contrast to other genes, however, GHR showed a less significant difference in our specimens (Figure 4j).

### IHC Results

Quantitative real-time PCR results prompted us to further explore the expression levels of TLE1, BCL2,

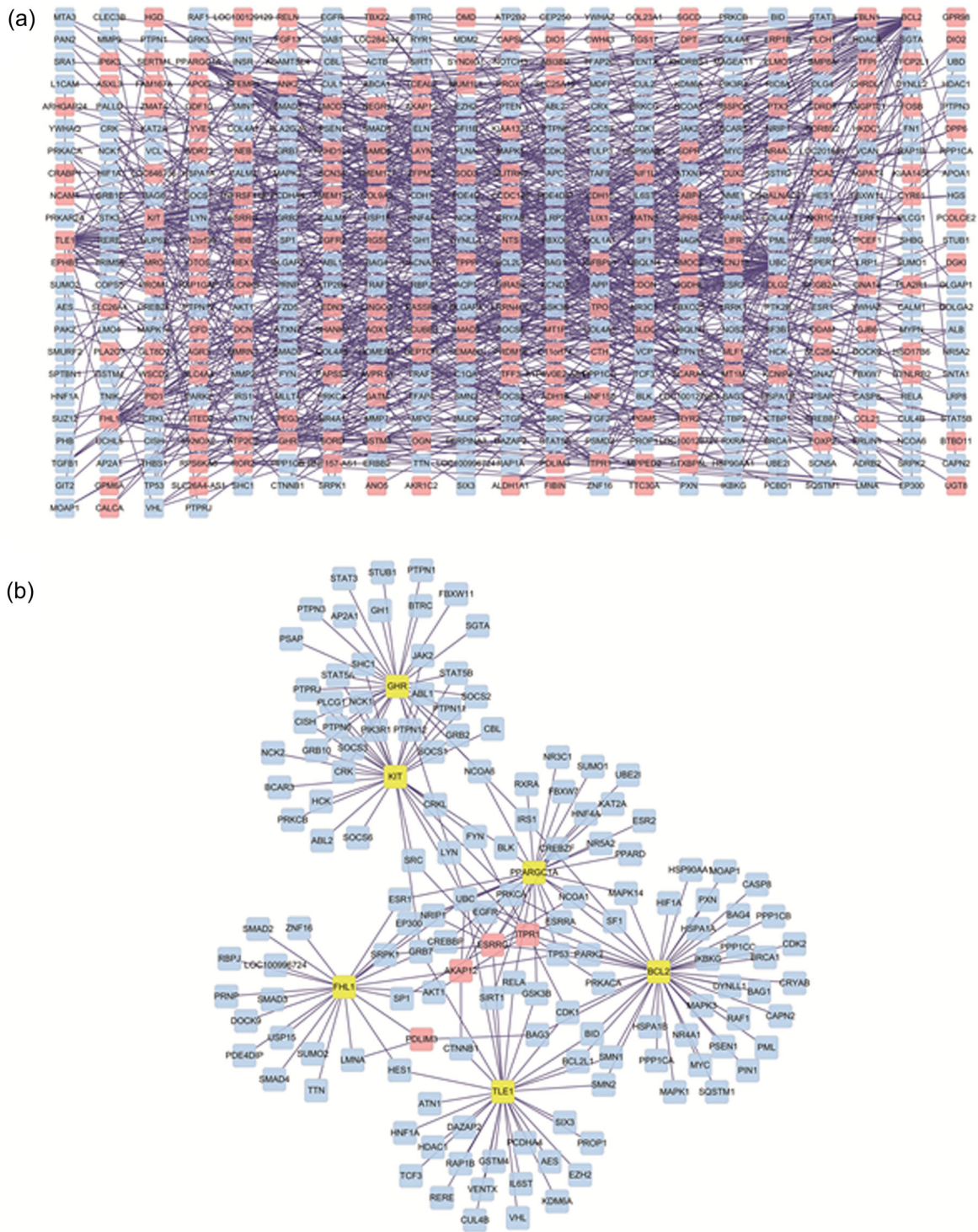


**FIGURE 3** Protein–Protein interaction (PPI) network was visualized using the BisoGenet software based on the database, including BIND, DIP, HPRD, RefSeq, SwissProt and IPI and so forth. (a) PPI network of down-regulated DEGs with neighbor nodes. (b) Core PPI network of the hub genes with neighbor nodes (cutoff  $\geq 25$ ). Red color represents the DEGs. Blue color represents the neighbor nodes in the PPI network. And Yellow color represents the hub genes of down-regulated DEGs. BIND, binding database; DEG, Differentially expressed genes; DIP, database of interacting protein; HPRD, Human Protein Reference Database.

FHL1, KIT, GHR, and PPARGC1A in human PTC tissues via immunohistochemical staining. The clinical, histopathological, and immunohistochemical profiles of the patients are detailed in Table 1. The cohort comprised 19 females (63.3%) and 11 males

(36.7%) diagnosed with PTC, with an average age of 44.8 years (SD  $\pm$  14.7). Immunohistochemical analysis showed a strong nuclear and cytoplasmic presence of FHL1 in normal thyroid tissues adjacent to tumors, whereas it was notably absent in PTC tissues

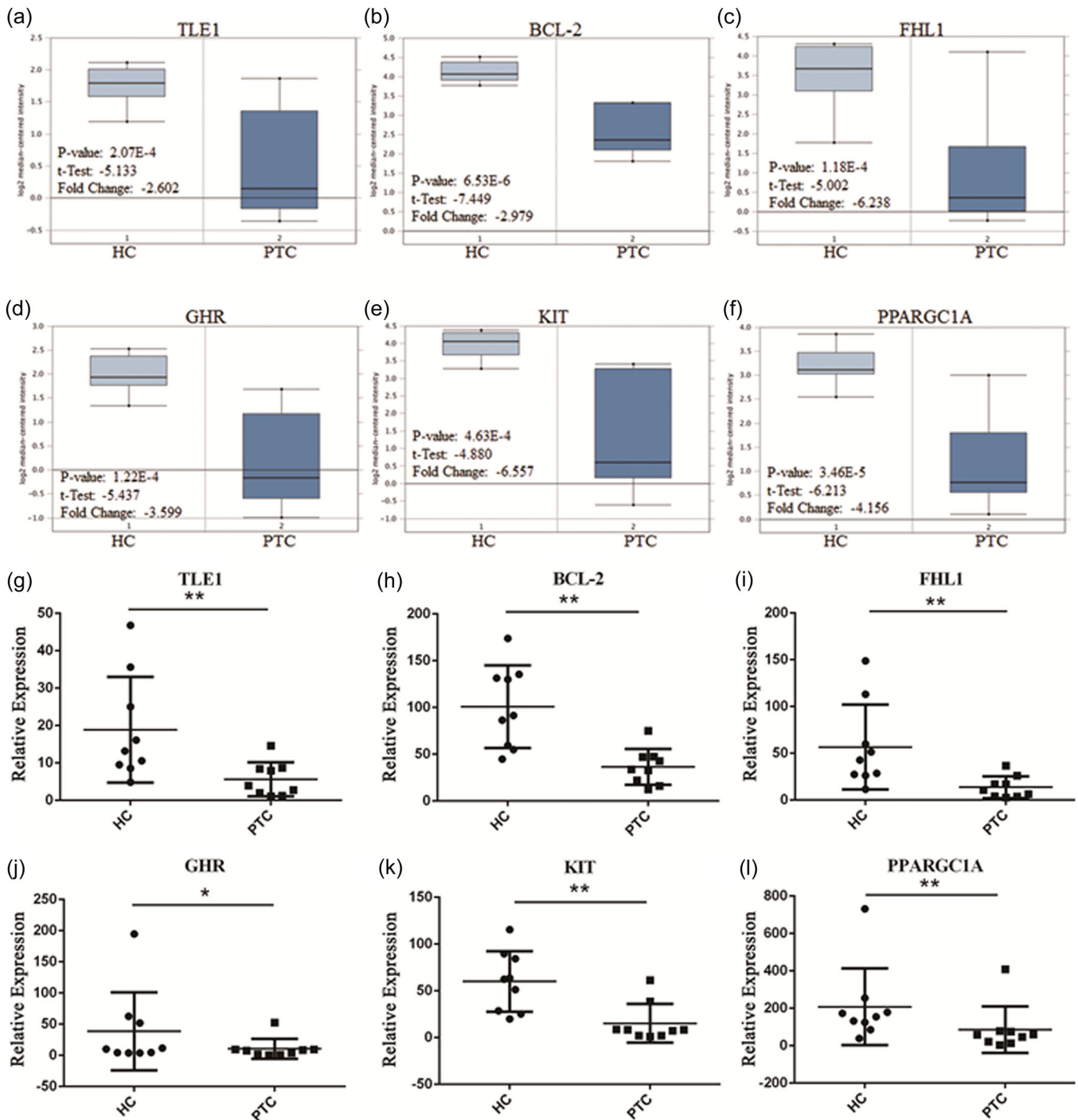


**FIGURE 4** mRNA expression of hub genes. (a–f) Hub genes expression analysis in papillary thyroid carcinoma (ONCOMINE database). Box plots showed gene expression data of PTC tissue compared with that of the normal thyroid in ONCOMINE. The  $p$  Value was set up at 0.05 and fold change was defined as 2. The y-axis represents log<sub>2</sub> median-centered intensity (normalized expression). (g–l) Q-PCR analysis of hub genes transcription in PTC. RNA extracted from 30 pairs of PTC and adjacent nontumor tissue samples was used. \* $p < 0.05$ , \*\* $p < 0.01$ . mRNA, messenger RNA; Q-PCR, quantitative real-time polymerase chain reaction.

( $p < 0.01$ ) In contrast, BCL2 expression did not significantly differ between PTC and adjacent normal thyroid tissues ( $p > 0.05$ ). Intriguingly, TLE1, KIT, PPARGC1A, and GHR were undetectable in both

tumor and normal tissues (Figure 5). In addition, we have conducted IHC testing on three fine-needle aspiration (FNA) specimens. Two of them showed weak positive expression of FHL1 (Figure S1A–B).

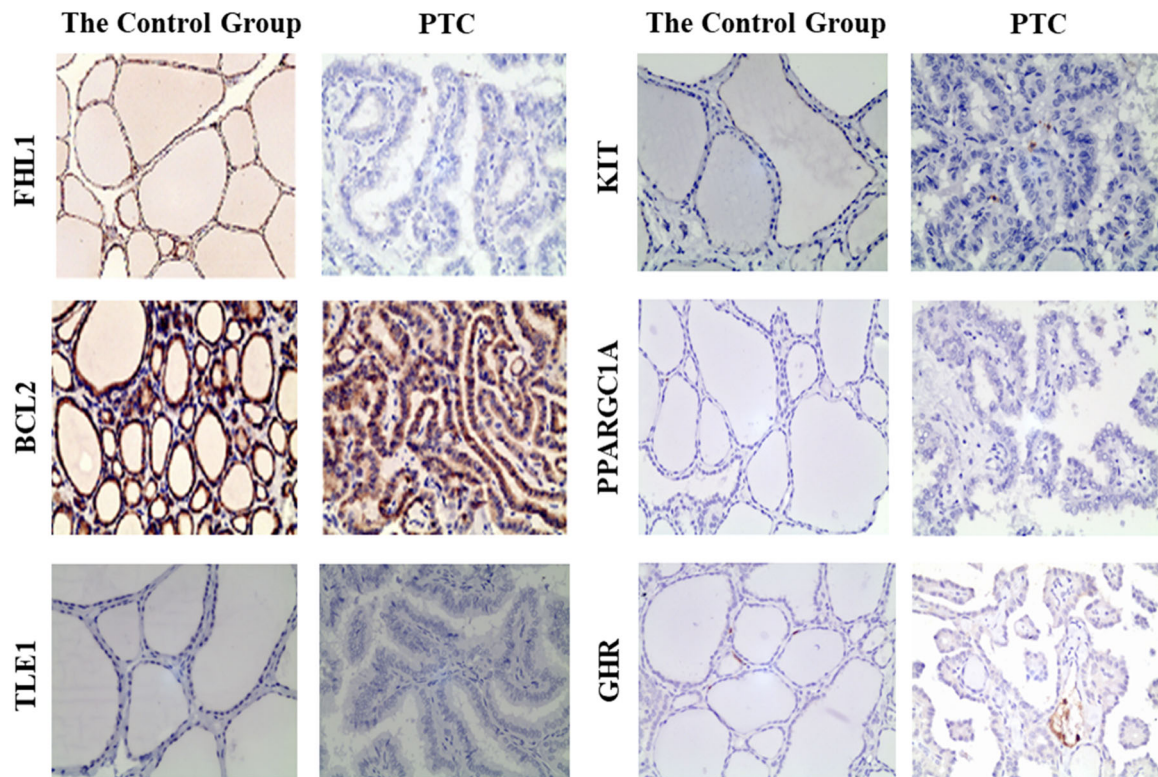


**FIGURE 5** The expression of FHL1, BCL2, TLE1, KIT, PPARGC1A and GHR in papillary thyroid carcinoma (PTC) and the control group. FHL1 showed strong positivity in the nuclei and to a lesser extent in the cytoplasm of normal thyroid tissues adjacent to the tumour (the control group), but is not present in the PTC tissues. ( $p < 0.01$ ). There was no significant difference in the expression of BCL2 between PTC and normal thyroid tissues ( $p > 0.05$ ). The results showed that TLE1, KIT, PPARGC1A, and GHR were absent in both tumor and normal tissues. (magnification  $\times 200$ ). FHL1, four and a half LIM domains 1.

## DISCUSSION

While there are established morphological criteria for diagnosing PTC, distinguishing these features, particularly in fine needle aspiration and biopsy specimens, remains challenging. Immunohistochemical staining is valuable for differential diagnosis. In this research, we leveraged bioinformatics to identify several hub genes linked to PTC. PCR and IHC results indicated that FHL1 expression was down-regulated in PTC tissues.

This study undertook a comprehensive gene expression profile analysis to pinpoint candidate genes that could act as reliable molecular markers for diagnosing PTC. By integrating microarray data from 108 samples, including 56 PTC specimens and 52 normal thyroid tissues, we identified 429 DEGs—237 were up-regulated and 192 down-regulated. Our focus was particularly on the down-regulated genes given their potential role in PTC pathogenesis. The thyroid gland's critical role in regulating body metabolism is well-documented.<sup>9</sup> Accordingly, GO and pathway enrichment analyses revealed that down-regulated DEGs were predominantly associated with thyroid hormone synthesis and protein metabolism, suggesting these pathways may be crucial in PTC oncogenesis. Further, we identified six hub genes—TLE1, BCL2, FHL1, GHR, KIT, and PPARGC1A—through

data mining. The mRNA expressions of these genes were consistent with microarray data. Immunohistochemical staining was used to examine the expression of these genes in human PTC tissues. Our findings revealed strong nuclear and moderate cytoplasmic expression of FHL1 in normal thyroid tissues surrounding tumors, whereas it was absent in PTC tissues. Interestingly, BCL2 expression did not significantly differ between PTC and normal thyroid tissues ( $p > 0.05$ ). The four other markers, TLE1, GHR, KIT, and PPARGC1A, were not detected in either PTC or normal thyroid tissues, indicating the need for further investigation into their roles.

It is reported that the immunohistochemical markers associated with PTC, such as thyroperoxidase, CK19, galectin-3, FN1,<sup>9</sup> CD56,<sup>10</sup> and HBME-1, play a role in thyroid carcinomas and have been widely described.<sup>3,11,20–22</sup> However, their diagnostic utility in PTC remains a subject of ongoing debate. The use of combined antibodies has shown improved diagnostic accuracy. Our findings indicate that immunohistochemical staining for FHL1 could be valuable in differentiating PTC and may be applicable to cytological specimens in future studies.

FHL1 is a subfamily of proteins within the LIM-only protein family.<sup>23</sup> It is reported that the expression of FHL1 is found in different tissues and plays a role in



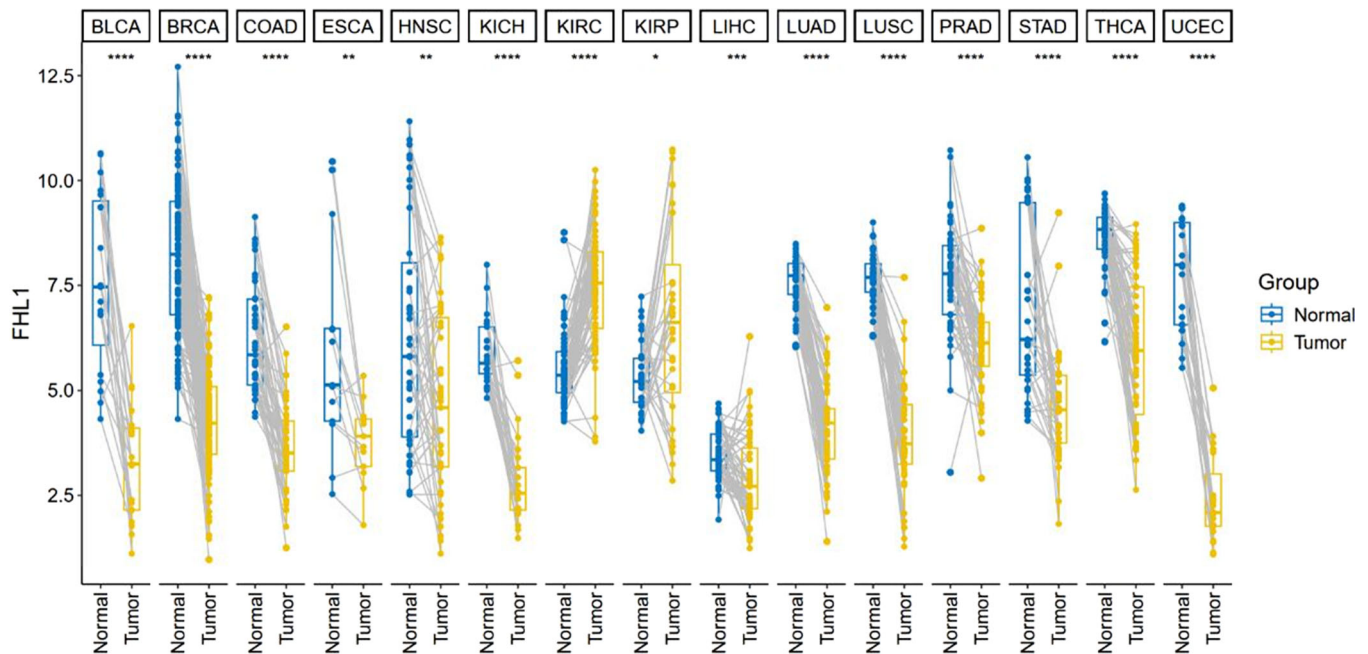


**FIGURE 6** The expression of FHL1 gene in pan-cancer from TCGA data. FHL1, four and a half LIM domains 1; TCGA, The Cancer GenomeAtlas Program.

various types of cancer, such as tongue squamous cell carcinoma,<sup>24</sup> gastric cancer,<sup>25</sup> esophageal squamous cell carcinoma,<sup>26</sup> lung cancer,<sup>27</sup> liver and colorectal tumors.<sup>28</sup> To investigate FHL1's role in carcinogenesis further, we analyzed its expression across 37 human cancers using the TCGA database. As depicted in Figure 6, FHL1 showed significant differential expression in 15 cancer types relative to normal tissues, including BLCA, BRCA, COAD, ESCA, HNSC, KIRC, KIRP, LIHC, LUAD, LUSC, PRAD, STAD, thyroid carcinoma, and UCEC. This underscores FHL1 is potential as a biomarker across a broad spectrum of cancers.

The diagnosis of PTC traditionally relies on distinctive nuclear features alongside papillary or solid/trabecular architecture, or infiltrative growth in follicular-patterned tumors. However, the emphasis on nuclear features is increasingly being supplanted by molecular diagnostics.<sup>29</sup> Molecular mechanisms in PTC are predominantly linked to mutations in oncogenes such as BRAF, RAS, RET, and TERT. These genetic alterations can result in varied biological behaviors and growth patterns of the tumor, underscoring the need for deeper exploration of PTC's molecular characteristics. FHL1, in particular, may serve as a promising biomarker for tumorigenesis.

This study, however, is not without its limitations. Firstly, we have assessed FHL1 immunostaining on FNA samples in a limited number of cases, which will be further discussed in subsequent research. Secondly, the introduction of noninvasive follicular thyroid neoplasm with papillary-like features (NIFTP) in 2016 as a noncancer entity poses challenges for thyroid FNA interpretation, particularly the cytological suspicion of NIFTP. Given the

limited availability of NIFTP data in the GEO database and its minimal representation in our study, it was not extensively discussed. Future studies could focus on this aspect. Thirdly, while this study did not experimentally explore the FHL1 gene mechanism, we did analyze the correlation between FHL1 expression and GSEA pathway analysis, warranting further detailed investigation.

In conclusion, this study pioneers the assertion that the dysregulation of FHL1 may be integral to the development and progression of PTC. FHL1 holds promise as a significant marker for accurate diagnosis and a prospective therapeutic target in PTC management. Nonetheless, the specific mechanisms underlying the dysregulation of FHL1 expression require further investigation. Future studies should explore the correlation between FHL1 expression levels and clinical variables, including age, gender, primary tumor size, disease stage, lymph node involvement, distant metastasis, and various histopathological types of thyroid cancer. Evaluating a larger cohort will enhance our understanding of thyroid cancer pathogenesis. Ultimately, our goal is to identify reliable biomarkers that not only clarify the pathogenic underpinnings of PTC but also facilitate precise diagnostics and personalized treatment approaches.

## AUTHOR CONTRIBUTIONS

**Yeting Zeng and Dehua Zeng:** Conceptualization, methodology, acquisition and analysis of data, writing-original draft, writing-review and editing, project administration. **Xingfeng Qi and Hanxi Wang:** Conceptualization, materials preparation and immunohistochemical experiments. **Xuzhou Wang and Xiaodong Dai:** Resources,

validation. **Yeting Zeng and Lijuan Qu:** Conceptualization, supervision, project administration, funding acquisition. All authors have read and agreed to the published version of the manuscript.

## ACKNOWLEDGMENTS

This work was supported by the Fujian Province clinical key specialty construction project [grant number 2015ZDZKBL].

## CONFLICT OF INTEREST STATEMENT

The authors declare no conflict of interest.

## ORCID

Yeting Zeng  <http://orcid.org/0000-0001-8996-3564>

## REFERENCES

- Fagin JA, Wells Jr. SA. Biologic and Clinical Perspectives on Thyroid Cancer. *N Engl J Med*. 2016;375(11):1054–67.
- Lloyd RV, Buehler D, Khanafshar E. Papillary thyroid carcinoma variants. *Head Neck Pathol*. 2011;5(1):51–6.
- Kaliszewski K, Diakowska D, Strutynska-Karpinska M, Rzeszutko M, Grzegorzolka J, Dziegiel P, et al. Expression of cytokeratin-19 (CK19) in the classical subtype of papillary thyroid carcinoma: the experience of one center in the Silesian region. *Folia Histochem Cytobiol*. 2017;54(4):193–201.
- Lee MY, Ku BM, Kim HS, Lee JY, Lim SH, Sun JM, et al. Genetic Alterations and Their Clinical Implications in High-Recurrence Risk Papillary Thyroid Cancer. *Cancer Res Treat*. 2017;49(4):906–14.
- Kimura ET, Nikiforova MN, Zhu Z, Knauf JA, Nikiforov YE, Fagin JA. High prevalence of BRAF mutations in thyroid cancer: genetic evidence for constitutive activation of the RET/PTC-RAS-BRAF signaling pathway in papillary thyroid carcinoma. *Cancer Res*. 2003;63(7):1454–7.
- Agrawal N, Akbani R, Aksoy BA, Ally A, Arachchi H, Asa SL, et al. Integrated genomic characterization of papillary thyroid carcinoma. *Cell*. 2014;159(3):676–90.
- Guan X, Wang P, Chi J, Zhao S, Wang F. Relationships of BRAF mutation and HMGB1 to papillary thyroid carcinoma. *Biochem Biophys Res Commun*. 2017;486(4):898–903.
- Franceschi S, Lessi F, Panebianco F, Tantillo E, La Ferla M, Menicagli M, et al. Loss of c-KIT expression in thyroid cancer cells. *PLoS One*. 2017;12(3):e0173913.
- Zhang H, Teng X, Liu Z, Zhang L, Liu Z. Gene expression profile analyze the molecular mechanism of CXCR7 regulating papillary thyroid carcinoma growth and metastasis. *J Experim Clin Cancer Res*. 2015;34(1):16.
- Abouhashem NS, Talaat SM. Diagnostic utility of CK19 and CD56 in the differentiation of thyroid papillary carcinoma from its mimics. *Pathol Res Pract*. 2017;213(5):509–17.
- Zhu X, Sun T, Lu H, Zhou X, Lu Y, Cai X, et al. Diagnostic significance of CK19, RET, galectin-3 and HBME-1 expression for papillary thyroid carcinoma. *J Clin Pathol*. 2010;63(9):786–9.
- Liu Z, Li X, Shi L, Maimaiti Y, Chen T, Li Z, et al. Cytokeratin 19, thyroperoxidase, HBME-1 and galectin-3 in evaluation of aggressive behavior of papillary thyroid carcinoma. *Int J Clin Exp Med*. 2014;7(8):2304–8.
- Guo W, Xie L, Zhao L, Zhao Y. mRNA and microRNA expression profiles of radioresistant NCI-H520 non-small cell lung cancer cells. *Mol Med Rep*. 2015;12(2):1857–67.
- Rhodes DR, Yu J, Shanker K, Deshpande N, Varambally R, Ghosh D, et al. ONCOMINE: a cancer microarray database and integrated data-mining platform. *Neoplasia*. 2004;6(1):1–6.
- Yuanyuan S, Qin S, Rongrong X, Yujing G, Chengbin P, Jianjun M, et al. Reference gene selection for real-time quantitative PCR analysis on ovarian cryopreservation by vitrification in mice. *J Assist Reprod Genet*. 2015;32(8):1277–84.
- Lloyd RV, Klöppel G. WHO Classification of Tumours of the Endocrine Organs, World Health Organization; 2017. p. 81–91.
- Abdulhaleem M, Bandargal S, Pusztaszeri MP, Rajab M, Greenspoon H, Krasner JR, et al. The Impact of BRAF V600E Mutation Allele Frequency on the Histopathological Characteristics of Thyroid Cancer. *Cancers*. 2023;16(1):113.
- Li Q, Li N, Zeng Y, Wang X, Li J, Su H, et al. Nuclear receptor FXR impairs SK-Hep-1 cell migration and invasion by inhibiting the Wnt/ $\beta$ -catenin signaling pathway. *Oncol Lett*. 2020;20(5):1.
- Savin S, Cvejic D, Isic T, Paunovic I, Tatic S, Havelka M. Thyroid peroxidase and galectin-3 immunostaining in differentiated thyroid carcinoma with clinicopathologic correlation. *Hum Pathol*. 2008;39(11):1656–63.
- Song S, Kim H, Ahn SH. Role of Immunohistochemistry in Fine Needle Aspiration and Core Needle Biopsy of Thyroid Nodules. *Clin Exp Otorhinolaryngol*. 2019;12(2):224–30.
- Ramkumar S, Sivanandham S. The Combined Utility of HBME-1 and Galectin-3 Immunohistochemistry and BRAF V600E Mutations in the Diagnosis of Papillary Thyroid Carcinoma. *Cureus*. 2021;13(12):e20339.
- Asghari A, Vosough Z, Khafri S, Sadr Moharrerpour S, Ghorbani H. Scoring System and Diagnosis of Papillary Thyroid Carcinoma Using Human Bone Marrow Endothelium Marker-1, Cytokeratin 19, and Galectin-3. *Med J Islam Repub Iran*. 2023;37:25.
- Cao CY, Mok SWF, Cheng VWS, Tsui SKW. The FHL2 regulation in the transcriptional circuitry of human cancers. *Gene*. 2015;572(1):1–7.
- Ren W, Lian P, Cheng L, Du P, Guan X, Wang H, et al. FHL1 inhibits the growth of tongue squamous cell carcinoma cells via G1/S cell cycle arrest. *Mol Med Rep*. 2015;12(3):3958–64.
- Xu Y, Liu Z, Guo K. Expression of FHL1 in gastric cancer tissue and its correlation with the invasion and metastasis of gastric cancer. *Mol Cell Biochem*. 2012;363(1–2):93–9.
- Ji C, Liu H, Xiang M, Liu J, Yue F, Wang W, et al. Downregulation of decorin and FHL1 are associated with esophageal squamous cell carcinoma progression and poor prognosis. *Int J Clin Exp Med*. 2015;8(11):20965–70.
- Niu C, Liang C, Guo J, Cheng L, Zhang H, Qin X, et al. Downregulation and growth inhibitory role of FHL1 in lung cancer. *Int J Cancer*. 2012;130(11):2549–56.
- Wang Y, Fu J, Jiang M, Zhang X, Cheng L, Xu X, et al. MiR-410 is overexpressed in liver and colorectal tumors and enhances tumor cell growth by silencing FHL1 via a direct/indirect mechanism. *PLoS One*. 2014;9(10):e108708.
- Bychkov A, Jung CK. What's new in thyroid pathology 2024: updates from the new WHO classification and Bethesda system. *J Pathol Transl Med*. 2024;58(2):98–101.

## SUPPORTING INFORMATION

Additional supporting information can be found online in the Supporting Information section at the end of this article.

**How to cite this article:** Zeng Y, Zeng D, Qi X, Wang H, Wang X, Dai X, et al. FHL1: a novel diagnostic marker for papillary thyroid carcinoma. *Pathol Int*. 2024;74:520–9. <https://doi.org/10.1111/pin.13467>